한국해안·해양공학회 학술발표논문집 (2009)
2009년 11월 5일-11월 6일
제18권, pp. 81-84

Improved Estimation of Directional Wave Spectrum using X-band Radar
X-밴드 레이다 영상을 이용한 파향 스펙트럼 측정 향상

Jeseon Yoo[1], Dong-Young Lee[2], Ki-Chun Jun[2] and Jong-Ju Yoon[3]
유제선[1], 이동영[2], 전기천[2], 윤종주[3]

1. INTRODUCTION

The spatial and temporal characteristics of ocean waves are quantified using continuous radar image sequences acquired by radar backscatters from the sea surface ripples drifting on longer waves. The longer waves modulate spatial patterns of the radar backscatters generated by interaction between the transmitted electromagnetic field and the ocean wind-induced surface ripples, leading to representation of ocean wave fields. Thereby, the backscattered signals in space and time domain as a proxy of actual ocean wave signals are used to calculate the directional wave spectrum (Borge and Soares, 2000).

Radar imaging of the wave fields is strongly dependent on the ocean wind (Izquierdo and Soares, 2005), since the backscattered patterns may not be obtained without the wind-induced surface ripples. Consequently, the marine X-band radar results in better representation of ocean wave characteristics during windy weather episodes (Keller and Wright, 1975; Plant and Keller, 1990; Lee et al., 1995). For this reason, the X-band radar has been applied to monitor coastal waves especially under extreme weather conditions which conventional *in situ* measurements can't fully cover due to the risk of instrumentation damages (Ziemer and Gunther, 1994).

Swell waves with relatively long wave periods and large wave heights approach coastal area, generally after or before storm events passing by. Since they propagate out of their generation fetch, swells appear smoother losing their rough surface ripples. Thus, the X-band radar rarely shows good performance for detecting large swell waves, receiving reduced radar backscatters from the swell surface.

In this study, a new radar processing approach to enhancively retrieve wave information from poor quality images is proposed. In particular, this research aims to improve estimation of directional wave spectrum using X-band radar images recorded when the swell waves dominate in the wave fields

2. Experimental Data

The X-band radar image sequences and *in situ* measurement data were collected in Hwajin (Pohang), located in the eastern coast of Korea, in December, 2004. Hydrodynamic data were collected in the water depth range of 4 to 25 m using *in situ* instruments such as pressure sensor, ADCP, and directional wave buoy. The radar image records were sampled at 0.74 Hz using the WaMoS II system mounted about 30 m above the mean water level. The radar collected 32 images per burst at every 10 minutes with the coverage of about 1.5 km from the antenna.

3. Methodology

3.1 Three Dimensional Fourier Analysis

The 3-D fast Fourier transform (3-D FFT) analysis is typically used to extract directional

1 발표자: 한국해양연구원 기후연안재해연구부 공학박사
2 한국해양연구원 기후연안재해연구부 책임연구원
3 한국해양연구원 기후연안재해연구부 연구원

wave power spectra from a 3-D radar image cube in which the spatial and temporal sea surface elevation information is stored (Borge and Soares, 2000; Borge et al., 2004). The 3-D FFT method transforms the spatial and temporal information consisting of pixel intensity values, $I(x,y,t)$, in the space (x,y) - time (t) domain to the spectral wavenumber - frequency domain:

$$|FFT(I(x,y,t))|^2 = \Phi(k_x, k_y, w) \qquad (1)$$

where k_x and k_y are the components of the wavenumber vector $\vec{k}$, ω is angular wave frequency, and Φ is the 3-D image energy spectrum. The spectral wave energy is distributed on the dispersion relation shell in the 3-D spectral wavenumber - frequency domain (i.e. Φ). The theoretical dispersion shell in the 3-D energy spectrum domain is defined with the condition of no surface currents as follows:

$$\omega = \sqrt{(g\vec{k}) \times \tanh(\vec{kh})} \qquad (2)$$

where the angular frequency ω can be rewritten as $2\pi f$ with wave frequency f (or the inverse of wave period $1/T$), g is gravitational acceleration, h is local depth. The wavenumber vector $\vec{k}$ has magnitude k which is defined as $2\pi/L$ where L is wavelength.

Since the 3-D FFT result is a 3-D matrix that includes 2-D wavenumber information for each layer of the resulted frequency bands, the 3-D energy spectrum is summarized in the form of ordinary directional spectrum in frequency and direction using the translation method suggested by Young et al. (1985):

$$E(f,\theta) = \frac{dk}{df} \int_w k\Phi(k_x, k_y, \omega) d\omega \qquad (3)$$

where E is 2-D energy spectrum in f-θ domain, and θ is wave direction.

3.2 Removal of Spurious Sea Clutter

Conspicuous ocean wave features in the radar image frame can be obtained during the presence of wind blowing over the sea. In contrast, the backscatter patterns start to be obscured when the wind gets weaker below a certain minimal limit (e.g. the wind speed > 3 m/s), revealing spurious clutter speckles. The spurious clutter speckles characterized by same intensity-level pixel groups appear scattered in all directions, while intermitted wave patches move with specific directions.

In order to eliminate the slowly drifting spurious speckles and retain wave features in directional motions, a backward image frame differencing scheme in time is applied to successive radar image frames (Lippmann and Holman, 1989). Here, the backward image frame differencing method is modified using three successive image frames rather than two frames to stably isolate and remove the random speckles:

$$dI_i = I_i - (I_i + I_{i-1} + I_{i-2})/3 \qquad (4)$$

where dI is a newly produced image after the image frame differencing, and i denotes the i^{th} image. Fig. 1(a) and (b) show an original radar image example recorded during swell waves and the backward frame differencing result, respectively. The area size selected here is 512 x 512 m.

Thereafter, a 2-D band-pass image filter is applied to each frame differenced image to remove the low and high frequency residual noise (to avoid confusion with the wave frequency, hereafter referred to as wavenumber) that still remains in the 2-D image domain. Image filtering in the wavenumber domain is conducted by the product of a 2-D FFT result of each frame-differenced image, $F(u,v)$, and a low-pass filter function, $H(u,v)$, where (u,v) = coordinates in the frequency domain. The lower and upper bounds for the band-pass filter are k_{in} = $2\pi/500$ and k_{out} = $2\pi/40$ rad/m, respectively.

The wave patches of interest appearing in the frame differenced image have a tendency to lead to higher energy values in one direction appearing in the 2-D FFT result. In order to retain these features and remove the residual noise scattered in all directions, a 2-D elliptic Butterworth filter, $G(u,v)$, is additionally applied in conjunction with the 2-D band-pass filter:

$$G(u,v) = \left[1 + \left(\frac{u \cdot \cos\Theta + v \cdot \sin\Theta}{k_M}\right)^2 + \left(\frac{-u \cdot \sin\Theta + v \cdot \cos\Theta}{k_m}\right)^2\right]^{-n} \qquad (5)$$

where Θ = angle of the major axis of the filter, k_M = cutoff wavenumber for the major axis, k_m = cutoff wavenumber for the minor axis, and n is filter order.

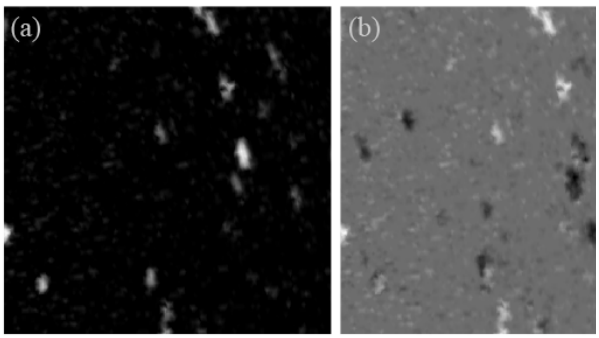

Fig. 1. (a) An example of original radar image captured from image, and (c) the filtered of (b) by Eq. 6.

The angle of the major axis, Θ, is determined from a linear regression of intensity values in the unfiltered 2-D FFT result. The energy threshold for the linear regression is set to be 0.4 in the normalized 2D FFT result by the energy maximum. The filtering factors k_M, k_m, and n are selected to be $2\pi/40$, $2\pi/80$, and 3, respectively. Thereby, the frame-differenced image is filtered in the wavenumber domain by the product of the 2-D FFT result, the 2-D band-pass filter, and 2-D elliptic Butterworth filter:

$$F_{filt}(u,v) = F(u,v) \bullet H(u,v) \bullet G(u,v) \qquad (6)$$

where $F_{filt}(u,v)$ is the filtered of $F(u,v)$ which is 2-D FFT result of the frame-differenced image. Fig. 1(c) shows the complete image after filtering of (b) by Eq. (6). The above additional processing steps are applied to each individual images prior to the 3-D FFT analysis of the whole image burst.

4. RESULTS AND DISCUSSION

The X-band radar image bursts with low signal-to-noise-ratio (SNR) recorded during the period of post-storm days were processed to remove the spurious speckles other than actual wave features using the procedure suggested above. The results of directional wave spectrum analysis from the processed radar image bursts were compared to the in situ measurements by an ADCP sensor deployed at about 20 m water depth.

Fig. 2 gives comparisons of the analysis results from an original image burst and the processed data burst. Due to the spurious artifacts scattering in all directions in the original image sequence, the original result contains high-level background noise energy for all directions and high frequencies (Fig. 2a and c). Meanwhile, the 2-D spectrum

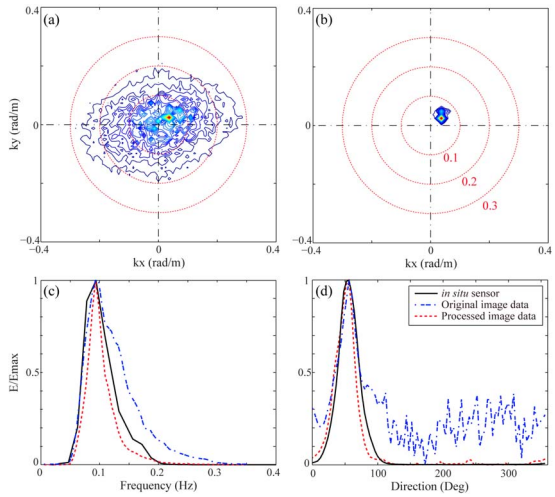

Fig. 2. (a) A 2-D wave spectrum in the wavenumber domain obtained from an original image data burst collected during swells, (b) the 2-D wave spectrum obtained from the processed data burst, (c) comparisons of frequency line spectra from in situ measurements and radar image data, and (d) comparisons of direction line spectra.

result of the processed one shows clear determination of the peak wavenumber and incident wave direction (Fig. 1b). Compared to the in situ measurements, the 2-D spectrum result of the processed image data lead to better agreements than that of the original image data (Fig. 2c and d).

5. CONCLUSION

The use of the marine X-band radar to monitor ocean surface waves is preferred under extreme weather conditions, while loses good observational quality in imaging the wave fields below a certain wind speed limit. Swells approaching to coastal area out of the generation fetch tend to be obscured in the radar image sequences due to less wind speed. Here, a new radar image processing method to reduce the spurious clutter speckles and enhancively retrieve directional wave spectrum from the swell radar images is proposed. The results of the directional wave spectrum computed through the suggested method were comparable to the *in situ* measurements.

ACKNOWLEDGEMENTS

This work was supported by the Korea Ocean Research and Development Institute (Grant PE98321).

REFERENCES

Borge, J.C., Rodriguez, R.G., Hessner, K. and Gonzales, I.P. (2004). Inversion of marine radar images for surface wave analysis. J. Atmos. Ocean. Technol., 21, 1291–1300.

Borge, J.C. and Soares, C. (2000). Analysis of directional wave fields using X-Band navigation radar. Coastal Eng., 40, 375–391.

Izquierdo, P. and Soares, C. (2005). Analysis of sea waves and wind from X-band radar. Ocean Eng., 32, 1404–1419.

Keller, W.C. and Wright, J.W. (1975). Microwave scattering and the straining of wind-generated waves, Radio Science, 10, 139-147.

Lee, P.H.Y., Barter, J.H., Beach, K.L., Hindman, C.L., Lake, B.M., Rungaldier, H. Shelton, J.C., Williams, A.B., Yee, R. and Yuen, H.C. (1995). X-Band microwave backscattering from ocean waves. J. Geophys. Res., 100(C2), 2591-2611.

Lippmann, T.C., and Holman, R.A. (1989). Quantification of sand bar morphology: a video technique based on wave dissipation. J. Geophys. Res., 94, 995–1011.

Plant, W.J. and Keller, W.C. (1990). Evidence of Bragg scattering in microwave Doppler spectra of sea return, J. Geophys. Res., 95(C9), 16 299-16310.

Ziemer, F. and Günther, H. (1994). A system to monitor ocean wave fields. Proc. 2nd Int. Conf. on Air-Sea Interaction and Meteorology and Oceanography of the Coastal Zone. Lisboa, September 22-27, 1994.